A Discrete Element Method Model of Corn Stalk and Its Mechanical Characteristic Parameters

Tao Zhang, Manquan Zhao, Fei Liu,* Haiqing Tian, Tuya Wulan, Yao Yue, and Dapeng Li

In a simulation model of the process of corn straw crushing, its physical parameters and the model itself influence the accuracy of the numerical calculations of the discrete element method. This study attempts to improve the simulation accuracy of the crushing process and to find the optimal combination of parameters. Based on the Hertz-Mindlin with Bonding contact model, multiple particle replacement and bonding programs written using Visual Studio were imported through the application programming interface (API) of a discrete element method (DEM) model to establish three particle-bonding materials for a numerical simulation of the crushing process. Using results of mechanical corn stalk tests, DEM simulations of impact fracture, compression fracture, and bending fracture were conducted to determine the optimal combination of parameters. The resultant DEM-parameter combination led to simulation errors of 3.83%, 5.95%, and 7.86% in numerical simulations of impact fracture, bending fracture, and compression fracture of corn stalks, respectively. The performance of the corn stalk DEM using the proposed optimal parameter combination was validated using a 9RS-60 corn stalk crusher, revealing that the numerical simulation error was 8.77%. This study can improve the accuracy of the discrete element method in the simulation of the corn straw breaking process.

Keywords: Corn straw; Discrete element method; Crushing; Parameter calibration

*Contact information: College of Mechanical and Electrical Engineering, Inner Mongolia Agricultural University, Hohhot 010018, P. R. China; *Corresponding author: afei2208@imau.edu.cn*

INTRODUCTION

Corn straw, a renewable biological resource left after the harvest of corn, has a wide range of applications that have not been fully explored, and corn stalks have not been fully utilized to date. Corn straw needs to be crushed before high-efficiency uses such as a livestock feed or fuel or being returned to the field as fertilizer (Zhang *et al*. 2018, 2020). Stalk crushers are typically used to convert the straw into livestock feed, but they have the disadvantages of high power consumption and low efficiency. At present, the research on the mechanism of corn stalk crushing is not thorough and has mostly focused on the crushing mechanism of a single stalk section in the crushing chamber. It is difficult to test the force on a corn stalk group and the corresponding movement pattern using experimental methods (Ma *et al*. 2016).

With improvements in computing technology, complex behavior information, such as the movement of particle groups, forces, and energy consumption during bulk material crushing, can be directly obtained from computer-aided numerical simulations and analysis with discrete element methods (DEMs) (Serna-Diaz *et al*. 2016). DEMs have been widely used in the design and optimization of agricultural machinery. For example, Han *et al*.

(2017) improved the work performance of an inside-filling air-blowing corn-seed-metering device; they calibrated the contact parameters of corn seed particle models through a simulation coupling the engineering discrete element method (EDEM) and computational fluid dynamics (CFD). Zhang *et al*. (2016) and Liu *et al*. (2016) obtained the movement pattern of corn seed groups in the seed chamber through DEM numerical simulation and optimized the structure and operating parameters of air-suction seed-metering devices. Many researchers have used DEM to simulate stalk movement.

Additionally, researchers have verified the accuracy of DEM and applied it in numerical simulations of straw particle motion (Liu *et al.* 2018; Zhang *et al*. 2019). These studies have revealed the interaction mechanism between straw and the machinery and provide a theoretical basis for improving the mechanical structure and optimization of operation parameters.

The DEM is used to simulate the crushing process of corn straw; it can easily obtain movement, force, and energy consumption. However, the existing stalk DEM models simulate the movement of objects formed by the bonding of single particles or single materials, even though some types of straw are not made of single materials; corn straw is composed of two or more types of materials. In this case, crushing simulations of objects formed by the bonding of single particles or single materials can have a relatively large error (Liu *et al*. 2015; Zeng *et al*. 2017, 2019a).

In this study, the physical parameters of corn stalks were first determined through an analysis of a Hertz-Mindlin-with-bonding contact model and mechanical tests. Next, the parameters were introduced into the EDEM for secondary development using Visual Studio software. Finally, a DEM model with calibrated parameters and composed of three types of materials was established to simulate the crushing process of natural air-dried corn stalks. The objective of this study was to establish a DEM of corn straw that can be crushed and to calibrate the parameters of the DEM to make the simulation more accurate and provide a basis for future simulation analysis.

EXPERIMENTS

Experimental Mechanical Tests of Corn Stalks

Mechanical tests of corn stalks can provide data as a basis for the establishment of a DEM model and calibration of the bonding parameters. To establish a corn straw DEM model, the mechanical parameters need to be tested and calibrated to include the normal stiffness, shear stiffness, critical normal stress, critical shear stress, bonding radius, and interparticle contact radius. The critical normal stress and shear stress of the material can be measured in tests. The normal stiffness, shear stiffness, bonding radius, and interparticle contact radius of the material are determined through calibration of the DEM simulation.

Therefore, tensile and shear tests were conducted to measure the critical, normal, and shear stress of the material. An impact fracture test, compression fracture test, and bending fracture test of the whole corn straw were performed to calibrate four DEM input parameters: normal stiffness, shear stiffness, bonding radius, and interparticle contact radius of the material. The instruments used for testing were a stalk impact fracturing tester (Droide, Beijing, China) and a microcomputer-controlled electronic universal testing machine (Droide, Beijing, China). The corn stalk samples used in the tests were taken from Hohhot (China) and were naturally air-dried and had a moisture content of 8.8%.

Impact Fracture Test of Corn Straw

During processing in a stalk crusher, corn stalks in the crushing chamber are impacted and fractured by a high-speed rotor. Therefore, reducing the DEM simulation error of impact fracturing can greatly improve the simulation accuracy of the corn straw crushing process. Energy consumption during impact fracturing was the basis for determining the bonding-parameter inputs for DEM simulations. In this study, the test measuring the energy consumption during impact fracturing of whole-length corn stalks was conducted using a stalk impact fracturing tester (Fig. 1).

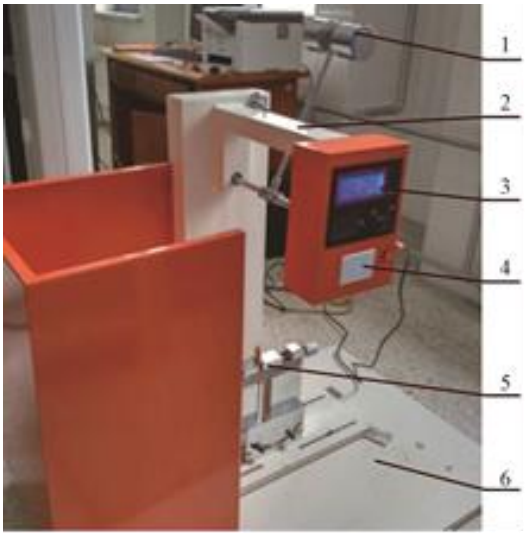

Fig. 1. Structure of straw impact fracture test machine: 1: Impact hammer; 2: Frame; 3: Data display screen; 4: Data printer; 5: Fixture; 6: Baseplate

It was assumed that an ear of corn grows from the 5^{th} node, that the 1^{st} to 4^{th} nodes are on the root side below the 5^{th} node, and that the 6^{th} to 10^{th} nodes are above the 5^{th} node (Fig. 2). (This assumption is based on the measurement of corn straw. The corn ear basically grows on the 5^{th} node.)

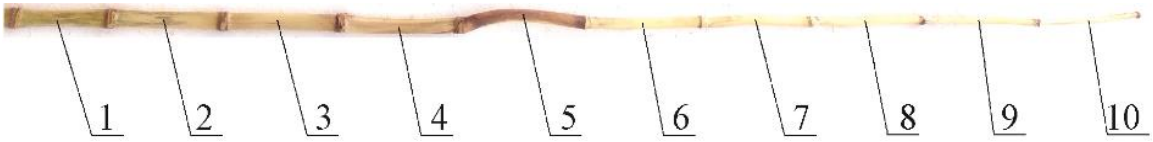

Fig. 2. The number of corn stalk internodes

To compare the mechanical properties of the internodes of a full-length corn stalk during impact fracturing in DEM, an impact fracturing test was conducted based on the cross-sectional area fractured on each internode. The energy consumption per unit cross-sectional area was then calculated. The test results are shown in Fig. 3.

As shown in Fig. 3, the impact fracture energy consumption per unit cross-sectional area of corn stalk decreased as the internode number increased. The energy consumption per unit cross-sectional area was higher from the 1^{st} to 5^{th} internode and lower from the 6^{th} to 10^{th} internode; the 6^{th} internode was remarkably lower than that of the 5^{th} internode, suggesting that the corn stalk section below the ear was mechanically stronger than the section above the ear.

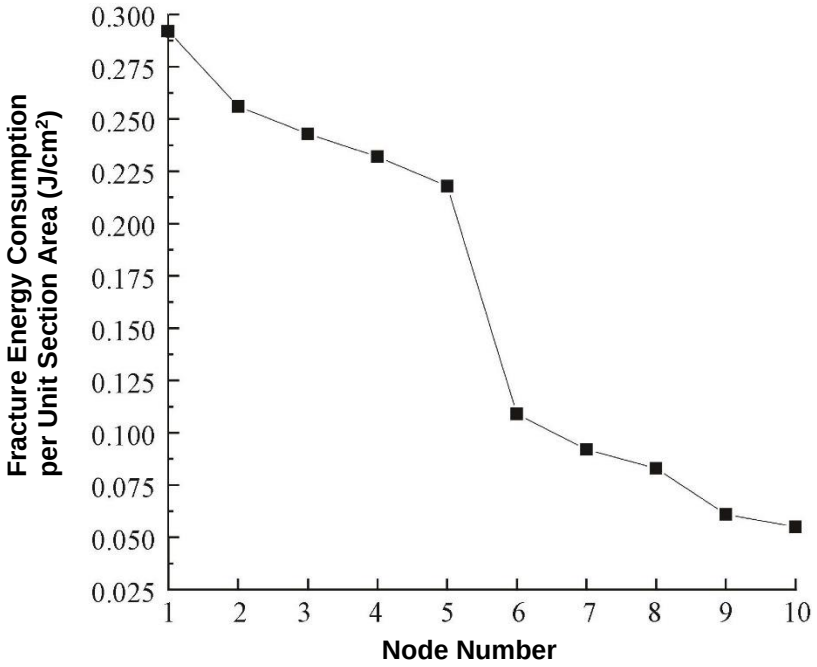

Fig. 3. Energy consumption test results of impact fracture of the corn straw unit cross-sectional area

According to the above analysis, the establishment of a corn stalk DEM simulation model requires two types of materials with different mechanical properties for the two parts of a corn stalk, *i.e.*, the lower part from the 1st to 5th internode on the root side and the upper part from the 6th to 10th internode.

Compared with the outer skin of the corn stalk, the inner pulp was mechanically weaker. The tensile and shear mechanical properties of the inner pulp differ slightly between the upper and lower parts, but those of the outer skin decreased as the internode number increased. Therefore, the corn stalk DEM simulation model required three types of materials to simulate the inner pulp, the upper outer skin, and the lower outer skin.

Tensile and Shear Tests of the Outer Skin and Inner Pulp of Corn Straw

Tensile and shear tests of the corn stalk inner pulp, the upper outer skin, and the lower outer skin, as well as compression and bending tests of the whole-length corn stalk, were conducted using a microcomputer-controlled electronic universal testing machine (Droide, Beijing, China). The results of the tensile and shear tests revealed that the mechanical properties of the outer skin were similar from the 1st to 5th internode and similar among all internodes above the 5th internode.

In this study, the average critical normal stress values of the lower outer skin, upper outer skin, and inner pulp of corn stalk were 1.418×10^8, 1.122×10^8, and 1.4×10^6 Pa, respectively, derived from 20 sets of testing results. The elastic modulus values (Young's modulus) of the lower outer skin, upper outer skin, and inner pulp, which were calculated based on the elastic deformation stages during the tensile tests of corn stalks, were 8.288×10^9, 6.356×10^9, and 1.664×10^8 Pa, respectively.

The maximum force during shear fracturing was obtained from a shear test using the shear test fixtures of the universal testing machine. Based on the maximum force and the cross-sectional area, the critical shear stress of the lower outer skin, the upper outer

skin, and the inner pulp of corn stalks were calculated as 1.243×10^7 Pa, 7.94×10^6 Pa, and 3.9×10^5 Pa, respectively.

Compression and Bending Test of the Whole Length of Corn Stalk

The cross-sections of corn stalks were approximately elliptical. Using the lengths of the long axis and short axis as size parameters of the cross-section, the mechanical properties during compression were measured using 10 lower corn stalk sections and 10 upper sections with moderate diameters. The corn stalk samples were all 40 mm in length; the average size of an elliptical cross-section of a corn straw lower sample was 23.06 mm (long diameter of ellipse) and 19.46 mm (short diameter), and that of an upper sample was 13.52 mm (long diameter) and 11.44 mm (short diameter). During testing, the speed of the pressing fixture was set at 10 mm/min; the simulation parameter setting was the same as the testing parameter setting. The average compression forces required for fracturing the lower and upper corn stalk sections were 2130 N and 960 N, respectively.

The mechanical properties under bending were tested using 10 lower and 10 upper corn stalk sections with moderate diameters. The samples were all 150 mm in length, the span of the bending fixture was 60 mm, and the pressing fixture was placed in the middle of the base fixture. The average lengths of the long and short axes of the cross-sections were 21.20 mm and 17.66 mm, respectively. The average size of the elliptical cross-section of a corn straw lower sample was 21.20 mm (long diameter of ellipse) and 17.66 mm (short diameter of ellipse), and that an upper sample was 13.46 mm (long diameter) and 11.38 mm (short diameter). During testing, the speed of the pressing fixture was set to 5 mm/min; the simulation parameter settings were the same as the testing parameter settings. The average bending forces required for fracturing the lower and upper corn stalk sections were 240 N and 110 N, respectively.

The compression force and bending force required for fracturing the corn stalks were compared with the DEM simulation results, laying a foundation for the calibration of corn stalk DEM parameters.

Establishment of a Corn Stalk DEM Model

The relationship between stress and strain of the inner pulp and outer skin of corn straw conforms to the generalized Hooke's law, and the fracture process is the same as that of a linear elastic-material model (Chen *et al.* 2012; Yu *et al*. 2012). Therefore, assuming that the material parameters of corn straw are linearly elastic, the Hertz-Mindlin with Bonding contact model was used to simulate the crushing of corn straw.

The Hertz-Mindlin with Bonding contact model is used to simulate problems such as breakage and fracture. Small particles are used to bond to bulk materials; the cohesive force between particles will be overcome under external force, to simulate the crushing process of materials. The energy consumption is calculated according to the force and displacement of the particle interaction in the process of bond fracture (Gao *et al*. 2020).

According to the above tests, a DEM simulation model of corn stalks must use three types of materials (lower outer skin, upper outer skin, and inner pulp of stalk). Therefore, three different materials were created by bonding particles in the same radius of 2 mm to establish a DEM model. The corn stalk DEM model was generated through a particle replacement and bonding process. A number of large particles were generated by a particle factory. Next, at the time of DEM simulation, an API program written in Visual Studio software (Microsoft Corporation, v. 2013, Redmond, WA, USA) started to run and use its plug-in program to read the coordinate positions of three types of particles, after the large

particles wrapping the entire stalk were replaced by the three types of small particles, the large particles were removed, the small particles were bonded at a preset time to form the corn stalk DEM model. The DEM model with three types of particles is shown in Fig. 4.

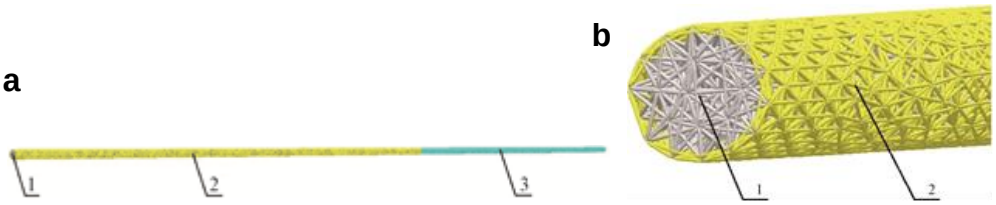

Fig. 4. Model of discrete element method simulation of corn stalk: a: model of whole corn stalk; b: roots of corn straw model

Figure 4 illustrates that the established DEM corn stalk simulation model includes, from inside to outside, the inner pulp, the contact between the inner pulp and the outer skin, and the outer skin. If the contact between the inner pulp and the outer skin has bonding mechanical parameters similar to the inner pulp, the established DEM model resembles a real corn stalk (Schramm *et al*. 2019; Zeng and Chen 2019b).

Calibration of the Bonding Mechanical Parameters for Corn Stalk Simulations

The contact parameters of the inner pulp and outer skin of the corn stalk were input into the established parameter combination. According to the analysis of the Hertz-Mindlin with Bonding contact model, the interparticle mechanical parameters that needed to be calibrated in a corn stalk DEM model include the normal stiffness, shear stiffness, critical normal stress, critical shear stress, bonding radius, and interparticle contact radius.

The measured results in the preceding tests were directly used as inputs of the critical normal stress and critical shear stress for the three types of materials simulating the upper outer skin, lower outer skin, and inner pulp of corn stalks. The DEM software was used to simulate the compression, bending, and impact fracturing of the corn stalks. The geometric size and speed of the main contact body in the simulation were the same as those in the test. The input parameters for the DEM simulation of the upper and lower corn stalk sections were calibrated. Multiple computer simulation calculations were performed with varying input parameters. After the simulation results of energy consumption of impact fracturing, bending force for fracturing, and compression force for fracturing were obtained through the postprocessing module of the DEM software, the values with a minimum average error were taken as input parameters in the simulation model.

The computer simulation of parameter calibration was conducted 91 times. The simulation error can be calculated by comparing the simulation results with the testing results. Through adjusting the input parameter combination multiple times, the combination that led to a minimum deviation between the simulation results and the testing results was considered the final calibrated result.

Among all the input parameters, the bonded-disk radius, the particle contact radius, and normal stiffness have a great influence on the simulation results. When the bonded-disk radius increases, the impact fracture energy consumption, bending fracture force, and compression fracture force increase; with the increase in the contact radius between particles, the corn straw toughness increases.

Numerical Simulation of Impact Fracturing of Corn Stalks

The proposed corn stalk DEM model simulates the crushing process of corn stalks. The crusher (9RS-600; Muchang Machinery, Zhengzhou, China) fractures and crushes the corn stalks through the rotation of a hammer plate. For the DEM simulation model to calculate the energy consumptions of fracturing the lower and upper stalk sections, the energy consumption of impact fracturing of the corn stalk model needs to be calibrated. The lengths of the long and short axes of the corn stalk samples used in the simulation model were the same as those in the impact test, as were the geometrical dimensions of the impact hammer, the corn stalk height protruding from the base fixture, the impact site of the corn stalk sample, and the position of the rotation axis of the impact hammer.

The impact fracturing process of the DEM simulation was the same as that in the test, as shown in Fig. 5. The API program was used for particle replacement and bonding. After particle replacement, interparticle bonds were generated to simulate corn stalks, which were then subjected to impact fracturing caused by an impact hammer rotating around a fixed axis. Figures 5a and 5b illustrate the corn stalk model before and after the impact fracturing, respectively.

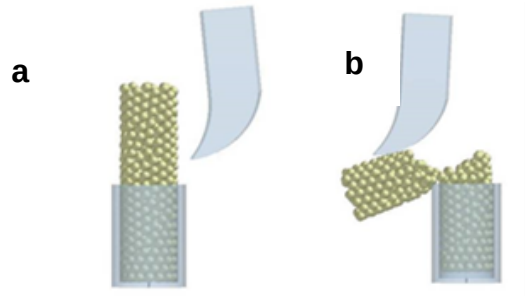

Fig. 5. Discrete element method simulation of corn stalk impact fracture: a: Before fracture; b: After fracture

The mechanical properties of the interparticle bonds were determined based on the normal stiffness, shear stiffness, critical normal stress, critical shear stress, bonding radius, and interparticle contact radius. The energy loss of the impact hammer under various parameter combinations was calculated using the postprocessing module of the DEM software according to the impact force on the corn stalk sample, the impact time, the displacement of the impact hammer, and the overlapping area between the impact hammer and the particles. The simulation error was obtained by comparing the energy loss of the impact hammer calculated by the DEM with that in the actual test. The formula used to calculate the error is proposed as Eq. 1,

$$\delta_1 = |M_1 - N_1| / M_1 \times 100 \quad (1)$$

where δ_1 is the calibration error of impact fracture in the DEM simulation (%), M_1 is the test value of energy consumption of the corn stalk impact fracture hammer, and N_1 is the simulation value of energy consumption of the hammer.

DEM Simulation of Corn Stalk Bending Fracture

The parameters related to bending fracture were input for calibration of the DEM model. The input geometrical model was the same as the bending fixture of the electronic universal testing machine used in the bending test. The DEM simulation of the bending

fracture is shown in Fig. 6. The simulated corn stalk was placed between the pressing and base rods prior to the bending test (Fig. 6a) and was bent and fractured as the pressing rod above the stalk moved downward at a constant speed (Fig. 6b).

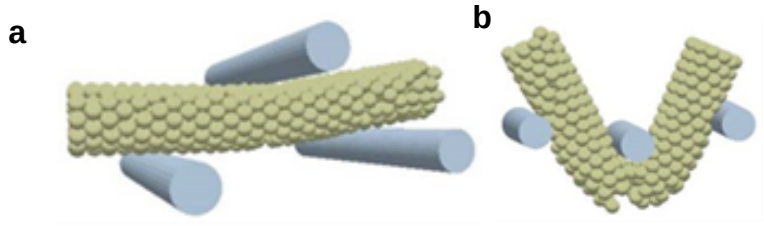

Fig. 6. Discrete element method simulation of corn stalk bend fracture: a: Before bending fracture; b: After bending fracture

After simulation, the force-displacement curve of the pressing rod was generated by the postprocessing module of the DEM software, and the calibration error of the DEM bending simulation was calculated according to the bending force during fracturing. The method of calculating the error of the bend fracture force was the same as above.

DEM Simulation of Corn Straw Compression Fracture

The parameters related to compression fracture were input for the DEM calibration. The input geometry model was the same as the compression fixture of the electronic universal testing machine used in the compression test. Figure 7 diagrams the DEM simulation of compression fracturing. The "corn stalk" was placed between the pressing plate and the base plate prior to the compression test (Fig. 7a); it was compressed and fractured as the upper pressing plate moved downward at a constant speed (Fig. 7b).

Fig. 7. Discrete element method simulation of corn stalk compression fracture: a: before compression fracture; b: after compression fracture

After simulation, the force-displacement of the pressing plate was generated by the postprocessing module of the DEM software. The calibration error between the DEM simulation and the testing results was analyzed based on the compression force that resulted in a fracture. The calculation of the error value of the bend compression fracture force was the same as above.

RESULTS AND DISCUSSION

Calibration of Bonding Parameters for the Corn Stalk DEM Simulation

The six bonding parameters in the DEM calibration include the normal stiffness, shear stiffness, critical normal stress, critical shear stress, bonding radius, and interparticle contact radius. Calibration of the corn stalk DEM models included the parameters related

to the following bonding: 1) between the lower outer skin particles, 2) between the lower outer skin and the inner pulp particles, 3) between the inner pulp particles, 4) between the lower and upper outer skin particles, and 5) between the upper outer skin particles.

The particle contact radius at the time of bonding determines the number of bonds that can be formed, which affects the overall mechanical properties of the DEM model. The normal stiffness and shear stiffness determine the mechanical properties of the model before fracturing of the bonds. The particle contact radius, critical normal stress, and critical shear stress after the formation of the bonds determine if the bonds are fractured.

According to the measured data from the mechanical-property tests of the lower outer skin, upper outer skin, and inner pulp, the critical normal stresses were 1.418×10^8, 1.122×10^8, and 1.4×10^6 Pa, respectively, and the critical shear stresses were 1.243×10^7, 7.94×10^6, and 3.9×10^5 Pa, respectively. In the DEM calibration, the measured parameters were input as fixed values without any adjustments. The particle radius, particle contact radius before bond formation, and particle contact radius after bond formation calculated with the simulation model were fixed.

The calibration process was as follows: First, a set of input parameters with relatively small errors were identified through impact fracture DEM calibration. This combination was then subjected to the DEM calibration of bending fracture and compression fracture. After adjustment, impact fracture DEM calibration was performed again until the simulations of impact fracture, bending fracture, and compression fracture had small errors.

The calibrated bonding parameters of the corn stalk DEM model are shown in Table 1. The bonded-disk radii were all set to 1.1 mm, the particle contact radius at the time of bonding was 4 mm, and the particle contact radii after bonding were all set to 6 mm.

Table 1. Calibration Results of the Discrete Element Method Simulation of Corn Straw Stalk Bonding Mechanical Parameters

Parameter	Calibration Results			
	Normal Stiffness Per Unit Area (N/m^3)	Shear Stiffness Per Unit Area (N/m^3)	Critical Normal Stress (Pa)	Critical Shear Stress (Pa)
Lower skin-Lower skin	5.5×10^9	5.5×10^8	1.4182×10^8	1.243×10^7
Lower skin-Inner pulp	5.05×10^8	5×10^7	1.4×10^6	3.9×10^5
Inner pulp-Inner pulp	5.05×10^8	5×10^7	1.4×10^6	3.9×10^5
Upper skin-Upper skin	4.98×10^9	5×10^8	$1.121\ 8 \times 10^8$	7.94×10^6
Upper skin-Inner pulp	5.05×10^8	5×10^7	1.4×10^6	3.9×10^5
Lower skin-Upper skin	4.98×10^9	5×10^8	$1.121\ 8 \times 10^8$	7.94×10^6

Error Analysis of the DEM Calibration Results

Table 2 presents the DEM simulation results when using the input parameter combination described above, the test results, and the errors regarding the impact fracture, bending fracture, and compression fracture of corn stalks.

Table 2. Comparison of Error Amounts between Simulation and Test Results

Node Number	Impact Fracture Energy Consumption (J)			Bending Fracture Force (N)			Compression Fracture Force (N)		
	Test	Simulation	Error (%)	Test	Simulation	Error (%)	Test	Simulation	Error (%)
2	3.92	4.1	4.59	242	238	1.65	2 366	2 468	4.31
2	3.61	3.75	3.88	255	241	5.49	2 293	2 408	5.02
2	3.75	3.7	1.33	259	249	3.86	2 256	2 116	6.21
4	2.95	2.85	3.39	221	230	4.07	1 821	1 916	5.22
4	3.12	3.22	3.21	215	222	3.26	1 788	1 658	7.27
4	2.81	2.99	6.41	206	215	4.37	1 755	1 911	8.89
6	1.32	1.31	0.76	140	130	7.14	1 100	1 254	14.00
6	1.41	1.46	3.55	143	128	10.49	1 058	975	7.84
6	1.48	1.53	3.38	138	129	6.52	1 043	1 152	10.45
8	0.7	0.65	7.14	109	118	8.26	850	781	8.12
8	0.75	0.79	5.33	115	126	9.57	832	763	8.29
8	0.68	0.7	2.94	105	112	6.67	835	762	8.74
Average Error			3.83			5.95			7.86
Root mean square error	4.22%			6.47%			8.26%		

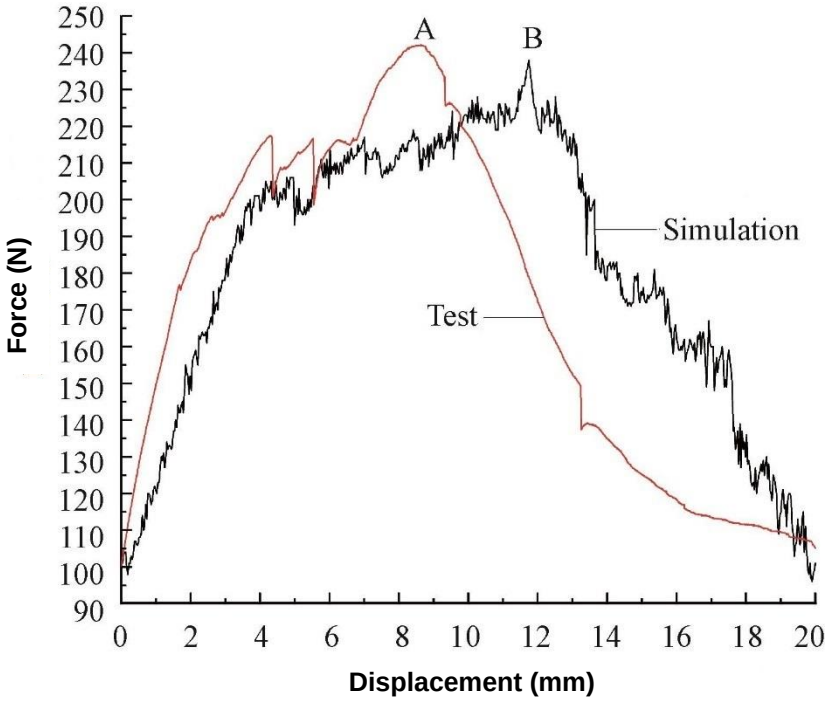

Fig. 8. Force-displacement curve of bending process for discrete element simulation and experiment. Point A is the maximum force of bend fracture (242 N); Point B is the maximum force of bend fracture during the discrete element simulation (238 N)

The average DEM simulation errors in energy consumption during impact fracturing, bending force for fracture, and compression force for fracture were 3.83%, 5.95%, and 7.86%, respectively. The force-displacement curves during the bending processes in the DEM simulation and test are shown in Fig. 8, and the force-displacement curves of the compression processes in the DEM simulation and test are shown in Fig. 9.

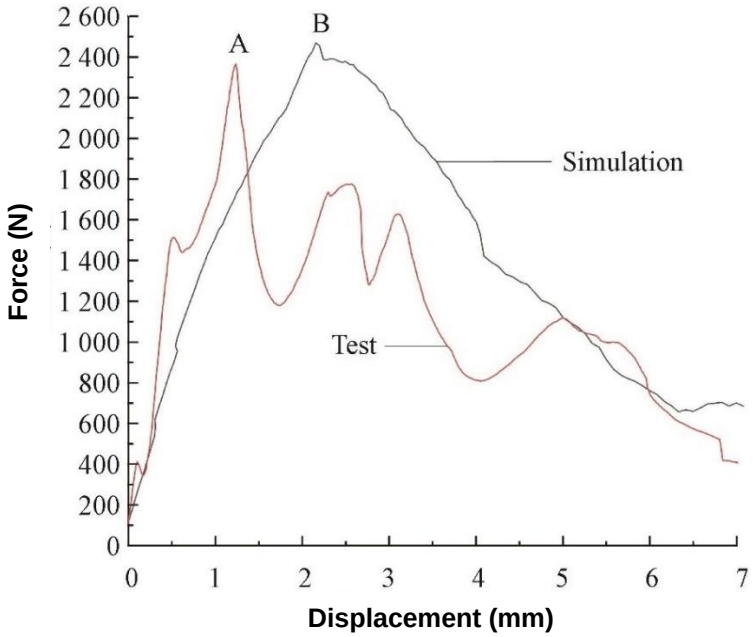

Fig. 9. Force-displacement curve of compression process for discrete element simulation and experiment; Point A is the maximum force of compression fracture during the test (2366 N); Point B is the maximum force of compression fracture during the discrete element simulation (2468 N)

As Figs. 8 and 9 show, the DEM simulation and the test yielded force-displacement curves with similar trends during the bending and compression processes. In particular, the maximum forces required for fracturing a corn stalk were close in the two scenarios, indicating a small simulation error. However, the displacement of the pressing mechanism at the time of compression-caused fracture and bending-caused fracture was greater in the DEM simulation than in the test, which was caused by the larger contact radius in the DEM simulation. The higher setting of the contact radius in the simulation was to ensure that the breaking of the interparticle bonds was caused by a force on the bonds exceeding the set critical normal and shear stresses, rather than exceeding the contact radius during the bending and compression processes.

As shown in Fig. 9, during the compression test of corn straw, the phenomenon of straw-skin splitting makes the force/displacement curve fluctuate; the force/displacement curve in the simulation process is relatively smooth. There are some differences between simulation and experiment. In this study, the DEM was used to simulate the crushing process of corn stalks by high-speed rotors in crushers. The maximum fracturing force can directly affect the simulation accuracy, while the geometric displacement of the pressing mechanism had little influence on the results. After the compression fracture of corn straw, the relationship between force and displacement has little influence on the accuracy of energy consumption simulation results. Therefore, the calibrated parameter combination can be applied in DEM simulations and analysis of the corn stalk crushing process.

Experimental Validation

The DEM model established in this paper was used to simulate the crushing process (Fig. 10). The crushing performance test of corn stalks was conducted on the 9RS-600 stalk crusher (Muchang Machinery, Zhengzhou, China) (Fig. 11). Six 1700 mm corn stalks were used in the experiment and simulation; the spindle speed was 1600 rpm as per GB/T 20788 (2006).

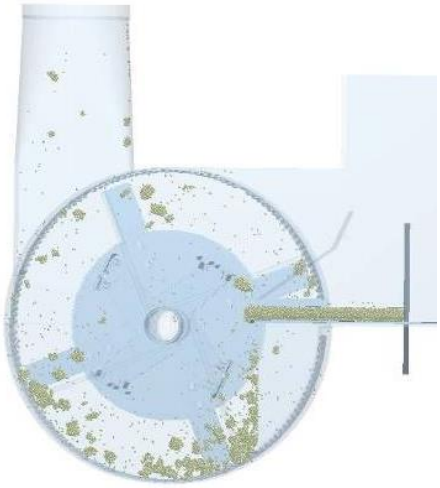

Fig. 10. Numerical simulation of crushing process of corn straw

Fig. 11. Crushing performance test of corn straw

The crushing process was video-recorded; the timing from the beginning of material feeding to the beginning of material discharge from the outlet was obtained by analyzing the video. The average time derived from three tests was 1.14 s.

The proposed DEM model in this study was used to numerically simulate the crushing process of corn stalks. The spindle speed was set to be the same as that in the test. The visualized and postprocessed data showed that the time from material feeding to discharging was 1.04 s. This result indicated that the validation experiment yielded a numerical simulation error of 8.77% in terms of the crushing time, confirming that the proposed DEM model can meet the requirements of numerical simulation.

CONCLUSIONS

1. In this study, the physical properties of natural air-dried corn straw were tested. The test results showed that the critical tensile stress values of the lower outer skin, upper outer skin, and inner pulp of corn stalk were 1.418×10^8, 1.122×10^8, and 1.4×10^6 Pa, respectively, and the critical shear stresses were 1.243×10^7, 7.94×10^6, and 3.9×10^5 Pa, respectively. The compression forces required for fracturing the lower and upper corn stalk sections were 2130 N and 960 N, respectively, and the bending fracture forces were 240 N and 110 N, respectively.
2. A DEM model for numerical simulation of the corn straw was established, and the parameters of normal stiffness, shear stiffness, critical normal stress, and critical shear stress were calibrated. It was found that the bonded-disk radius, particle contact radius,

and normal stiffness greatly influence the simulation results of energy consumption. The calibration results were as follows: the input parameters of the lower outer skin were 5.5×10^9 N/m^3, 5.5×10^8 N/m^3, 1.4182×10^8 Pa, and 1.243×10^7 Pa, respectively, the input parameters of the upper outer skin were 4.98×10^9 N/m^3, 5×10^8 N/m^3, 1.1218×10^8 Pa, and 7.94×10^6 Pa, respectively, and the input parameters of the inner pulp were 5.05×10^8 N/m^3, 5×10^7 N/m^3, 1.4×10^6 Pa, and 3.9×10^5 Pa, respectively. The errors of impact fracture, bending fracture, and compression fracture of corn straw were 3.83%, 5.95%, and 7.86%, respectively.

3. The crushing performance test of corn stalks was conducted on a 9RS-60 stalk crusher. The experimental results showed that the error of numerical simulation was 8.77%. Therefore, the established DEM and calibrated parameters can simulate the crushing process of corn straw.

ACKNOWLEDGMENTS

This research was funded by the National Natural Science Foundation of China (Grant Nos. 51665047 and 51765055) and the Fund for Introduction of High Level Talents in Inner Mongolia Agricultural University (No. NDYB2018-39).

REFERENCES CITED

Chen, Z., Wang, D., Li, L., and Shan, R. (2012). "Experiment on tensile and shearing characteristics of rind of corn stalk," *Transactions of the Chinese Society of Agricultural Engineering* 28(21), 59-65. DOI: 10.3969/j.issn.1002-6819.2012.21.009

GB/T 20788 (2006). "Tearing choppers," Standardization Administration of China, Beijing, China.

Gao, W., Liu, X., Chen, S., Bui, T. Q., and Yoshimura, S. (2020). "A cohesive zone based DE/FE coupling approach for interfacial debonding analysis of laminated glass," *Theoretical and Applied Fracture Mechanics* 108, 102668. DOI: 10.1016/j.tafmec.2020.102668

Han, D., Zhang, D., Jing, H., Yang, L., Cui, T., Ding, Y., Wang, Z., Wang, Y., and Zhang, T. (2018). "DEM-CFD coupling simulation and optimization of an inside-filling air-blowing maize precision seed-metering device," *Computers and Electronics in Agriculture* 150, 426-438. DOI: 10.1016/j.compag.2018.05.006

Hu, G. (2010). *Analysis and Simulation of Granular System by Discrete Element Method Using EDEM*, Wuhan University of Technology Press, Wuhan, China.

Liu, Y., Han, Y., Jia, F., Yao, L., Wang, H., and Shi, Y. (2015). "Numerical simulation on stirring motion and mixing characteristics of ellipsoid particles," *Acta Physica Sinica* 64(11), Article ID 114501. DOI: 10.7498/aps.64.114501

Liu, Y., Zhao, M., Liu, F., Yang, T., Zhang, T., and Li, F. (2016). "Simulation and optimization of working parameters of air suction metering device based on discrete element," *Transactions of the Chinese Society for Agricultural Machinery* 47(7), 65-72. DOI: 10.6041/j.issn.1000-1298.2016.07.010

Liu, F., Wang, W., Zhang, T., Ma, Q., and Zhao, M. (2018). "Air flow field numerical simulation and test of hammer rubbing machine," *Transactions of the Chinese Society for Agricultural Machinery* 49, 227-232. DOI: 10.6041/j.issn.1000-1298.2018.S0.030

Ma, Q., Liu, F., and Zhao, M. (2016). "Working mechanism and structure optimization of hammer of rubbing machine," *Transactions of the Chinese Society of Agricultural Engineering* 32(2), 7-15. DOI: 10.11975/j.issn.1002-6819.2016.z2.002

Schramm, M., Tekeste, M. Z., Plouffe, C., and Harby, D. (2019). "Estimating bond damping and bond Young's modulus for a flexible wheat straw discrete element method model," *Biosystems Engineering* 186, 349-355. DOI: 10.1016/j.biosystemseng.2019.08.003

Serna-Diaz, M. G., Arana-Cuenca, A., Medina-Marin, J., Seck-Tuoh-Mora, J. C., Mercado-Flores, Y., Jiménez-González, A., and Tellez-Jurado, A. (2016). "Modeling of sulfite concentration, particle size, and reaction time in lignosulfonate production from barley straw using response surface methodology and artificial neural network," *BioResources* 11(4), 9219-9230. DOI: 10.15376/biores.11.4.9219-9230

Yu, Y., Lin Y., Mao M., Wang, W., Tian, F., Pan, J., and Ying, Y. (2012). "Experimental study on tensile properties of corn straw," *Transactions of the Chinese Society of Agricultural Engineering* 28(6), 70-76. DOI: 10.3969/j.issn.1002-6819.2012.06.012

Zeng, Y., Jia, F., Zhang, Y., Meng, X., Han, Y., and Wang, H. (2017). "DEM study to determine the relationship between particle velocity fluctuations and contact force disappearance," *Powder Technology* 313, 112-121. DOI: 10.1016/j.powtec.2017.03.022

Zeng, Y., Jia, F., Xiao, Y., Han, Y., and Meng, X. (2019a). "Discrete element method modelling of impact breakage of ellipsoidal agglomerate," *Powder Technology* 346, 57-69. DOI: 10.1016/j.powtec.2019.01.082

Zeng, Z., and Chen, Y. (2019b). "Simulation of straw movement by discrete element modelling of straw-sweep-soil interaction," *Biosystems Engineering* 180, 25-35. DOI: 10.1016/j.biosystemseng.2019.01.009

Zhang, F., Song, X., Zhang, X., Zhang, F., Wei, W., and Dai, F. (2019). "Simulation and experiment on mechanical characteristics of kneading and crushing process of corn straw," *Transactions of the Chinese Society of Agricultural Engineering* 35(9), 58-65. DOI: 10.11975/j.issn.1002-6819.2019.09.007

Zhang, T., Liu, F., Zhao, M., Liu, Y., Li, F., Chen, C., and Zhang, Y. (2016). "Movement law of maize population in seed room of seed metering device based on discrete element method," *Transactions of the Chinese Society of Agricultural Engineering* 32(22), 27-35. DOI: 10.11975/j.issn.1002-6819.2016.22.004

Zhang, X., Feng, X., Zhang, H., and Wei, Y. (2018). "Utilization of steam-exploded corn straw to produce biofuel butanol *via* fermentation with a newly selected strain of *Clostridium acetobutylicum*," *BioResources* 13(3), 5805-5817. DOI: 10.15376/biores.13.3.5805-5817

Zhang, Y., Chen, H. T., Liu, S., Rokayya, S., and He, Y. Y. (2020). "Optimization of process parameters for preparing straw fiber from corn stalk rind," *BioResources* 15(1), 923-934. DOI: 10.15376/biores.15.1.923-934

Article submitted: July 21, 2020; Peer review completed: September 27, 2020; Revised version received and accepted: October 16, 2020; Published: October 23, 2020.
DOI: 10.15376/biores.15.4.9337-9350